Supporting Information

A very long-acting IL-15: Implications for the immunotherapy of cancer

John A. Hangasky[1], Wei Chen[2,†], Sigrid Dubois[2,†], Anusara Daenthanasanmak[2,†], Jürgen Müller[2], Ralph Reid[1], Thomas A. Waldmann[2*] and Daniel V. Santi[1*]

[1] ProLynx, San Francisco, CA, United States,
[2] Lymphoid Malignancies Branch, Center for Cancer Research, NCI, NIH, Bethesda, MD, United States

* Contributed equally
† Contributed equally

*Correspondence:
Thomas A. Waldmann, tawald@helix.nih.gov
Daniel V. Santi, daniel.v.santi@prolynxllc.com

Table of Contents

Figures and Tables

I. General Materials and Methods

Materials. Recombinant human IL-15 (>95% pure) was prepared as reported (*1*) and provided by the National Cancer Institute. RLI was produced at ATUM (Newark, CA) based on previously reported methods (*2, 3*). Mogamulizumab-kpkc (NDC code 42747-761-01) was obtained from the NIH Pharmacy. Anti-CD40 (#BP0016-2) was obtained from BioXCell (Lebanon, NH). C57B/6J plasma was purchased from Innovative Research (Novi, MI). All other chemicals and reagents were purchased from commercial vendors unless otherwise stated.

II. Analytical procedures for IL-15

HPLC analysis. HPLC analyses were performed on a Shimadzu LC-20AD HPLC system equipped with a Phenomenex Jupiter 5 µM C18 column (300 Å, 150 x 4.6 mm) heated to 40°C and a SPD-M20A photodiode-array detector. The elution program consisted of a 10-min linear gradient from 20- to 100% CH_3CN containing 0.1% TFA with a flow rate of 1 mL/min.

Mass spectrometry. Proteins were analyzed using LC/ESI-MS on a Waters Acquity UPLC connected to a Waters Xevo QToF mass spectrometer. The LC used a reversed-phase Acquity C4 column at 40ºC. Solvent A was 99.9% H_2O/0.1% HCO_2H and solvent B was 99.9% CH_3CN/0.1% HCO_2H(v/v); the elution program consisted of a linear gradient from 20- to 100%B over 1 minute using a flow rate of 400 µL/min.

Cell-based assays. A U2OS cell-based assay kit for IL-2Rβγ binding was performed according to the manufacturer's instructions (DiscoverX, Part #93-0998E3CP5). Briefly, cells were plated (100 µL, ~5,000 cells/well) in 96 well assay plates and grown for 48 hours at 37ºC, 5% CO_2. Cells were then treated with varying concentrations of the cytokine and incubated for an additional 6 hours at 37ºC, 5% CO_2. Treated cells were then incubated with a chemiluminescent substrate for 1 hour at ambient temperature in the dark prior to luminescence determination with a Spectramax i3 plate reader using a 250 ms integration time.

A CTLL-2 proliferation assay was performed as previously described (*4, 5*). Briefly, cells were cultured in RPMI-1640 medium (ATCC) supplemented with 2 mM L-glutamine, 1 mM sodium pyruvate, 10% fetal bovine serum, and 10% T-STIM with Con A. Prior to assaying, cells were washed three times with RPMI-1640 media containing 10% fetal bovine serum. A 96 well plate was seeded (50,000 cells/well; 100 µL) and incubated for 4 hours at 37ºC, 5% CO_2. A dilution plate containing the rhIL-15 samples in RPMI-1640 media containing 10% FBS was prepared by

10-fold serial dilutions to 2 ng/mL followed by 2 fold serial dilutions to 7.8 pg/mL. Diluted rhIL-15 samples (100 µL) were added to each well and incubated at 37ºC, 5% CO_2. Following a 48 hour incubation, CellTiter96 Aqueous One Solution was added (40 µL) and was incubated for three hours at 37ºC, 5% CO_2. The plate was then read at 490 nm using a Spectramax i3 plate reader.

ELISA. The rhIL-15 concentrations in serum were assessed using a hIL-15 specific ELISA (R&D Systems, hIL-15 Quantikine) performed according to the manufacturer's instructions. Plasma samples were thawed on ice prior to 10- or 50-fold dilution in the standard diluent. *h*IL-15 concentrations were plot as a function of time and fit using GraphPad Prism software.

Flow cytometry. PBMCs were prepared using ACK lysis buffer and incubated with a fixable viability dye to label dead cells. The FcRγII/II receptor was then blocked using CD16/32(2.4G2) (BD). PBMCs were surface stained using optimal Ab concentrations and then fixed for intracellular staining followed protocols from the eBioscience Foxp3/Transcription Factor Staining Buffer Set (ThermoFisher) (Table S1). Stained single cell suspension were analyzed on either FACScan (BD Biosciences) or Attune NxT flow cytometer (Thermofisher). FlowJo cytometry analysis software (TreeStar Inc, Ashland, OR) was used for data analysis. The absolute cell number was determined from complete blood count or by direct cell analysis (Attune NxT).

Table S1. Antibodies used for immunophenotyping.

Antibody	Clone	Vendor
αCD3e-FITC	145-2C11, 17A2	Invitrogen
αCD8a-PercP-Cy5.5	53-6.7	Invitrogen
αCD4-eFluor780	GK1.5	Invitrogen
αNK1.1-PE-Cy7	PK136	Invitrogen
αNK1.1-SuperBright600	PK136	Invitrogen
αCD44-APC	IM7	Invitrogen
αCD44-PE	IM7	Invitrogen
αKi67-APC	SolA15	Invitrogen
αCD19-APC-eFluor780	6D5	Biolegend
αCD19-eFluor450	1D3	Invitrogen
APC-eFluor780 Viability Dye	---	Biolegend
Live/Dead Fixable Aqua dead cell stain	---	Invitrogen
αCD335-PE	29A1.4	Biolegend
αhumanCD194-APC	L291H4	Biolegend
αhumanCD25-FITC	CD25-4E3	Invitrogen
TCRγ/δ-APC	ebioGL3	eBioscience

III. Preparation of MS~IL-15 conjugates

Optimization of azido-linker-IL-15 yield. In a total volume of 75 µL, reactions used 2.25 nmol (0.029 mg, 30 µM) IL-15 in 25 mM Citrate, pH 6.0, 500 mM NaCl and 0.05% tween-20 (Buffer A), 1.5- to 5 equivalents of N_3-PEG_4-L($MeSO_2$)-CHO (2 µg to 7 µg, 45 µM to 150 µM) and 750 nmol (47 µg,10 mM) $NaCNBH_3$. After 20 hours at room temperature, mixtures were treated with 0.5 mM DBCO-PEG_{5kDa} for 4 hours, and analyzed by SDS-PAGE. Here, DBCO-PEG_{5k} reacts with the azide of linker-IL-15 by SPAAC and slows migration (**Fig. S1**) (*6*).

A.

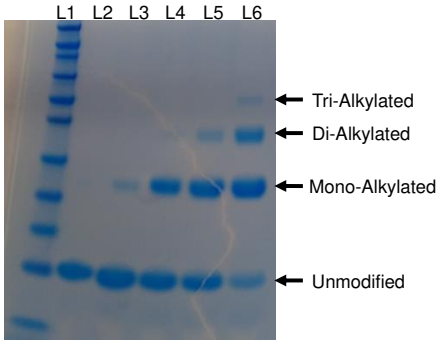

B.

Linker Eq.	% IL-15 Modification			
	Unmodified	Mono-Alkylated	Di-Alkylated	Tri-Alkylated
1.5	54	46	0	0
3	43	52	5	0
5	16	58	22	5

Figure S1. Reductive alkylation of IL-15. A) The progress of reactions were determined by SimplyBlue Safe-stained SDS-PAGE after SPAAC reaction of reductive alkylation mixtures (IL-15_{RM}) with DBCO-PEG_{5kDa}. SDS-PAGE of IL-15_{RM} performed with varying amounts of N_3-PEG_4-L($MeSO_2$)-CHO showing free-, mono- and multi-alkylated IL-15. IL-15 control or IL-15_{RM} (0.5 nmol) were treated with DBCO-PEG_{5kDa} (10 nmol) for 4 hours, then applied to the gel: L1, Novex Sharp Pre-Stained Protein Ladder; L2, IL-15 control; L3, IL-15 + PEG_{5KDa}; L4, N_3-linker:IL-15_{RM} = 1.0; L5, N_3-linker:IL-15_{RM} = 3.0; L6, N_3-linker:IL-15_{RM} = 5.0. B) Percent N_3-linker-IL-15 quantified from data in Panel A using ImageJ software. With 3 equivalents of N_3-linker, the reaction gave 52% IL-15 with 1 linker attached and 5% with two linkers attached. Increasing the N_3-linker to 5 equivalents gave a small increase in mono-alkylated IL-15, but 27% of the IL-15 had ≥two linkers attached.

Preparation of azido-linker-IL-15. In 64 mL of Buffer A, reaction mixtures contained 1.9 µmol (25 mg, 30 µM) IL-15, 5.8 µmol (3.3 mg, 90 µM) of N_3-PEG_4-L($MeSO_2$)-CHO and 640 µmol $NaCNBH_3$ (40 mg, 10 mM). The reaction was allowed to proceed 20 hours at ambient temperature in the dark, at which time the gel-shift assay indicated ~43% unreacted-, 52% monoalkylated- and 5% dialkylated-IL-15. The reaction mixture was concentrated to ~2 mL using an Amicon Ultra 3,500 MW cut-off concentrator and excess reagents were removed using a 14.5 x 50 mm PD-10 column (GE Healthcare) previously equilibrated in Buffer A. The reaction mixture was concentrated to ~1 mL using an Amicon Ultra 3,500 MW cut-off concentrator and the protein concentration (24 mg,

96% recovery) was determined by A_{280} (ε_{280}= 7240 M^{-1} cm^1) using a NanoDrop spectrophotometer.

In a similar fashion and with a similar yield, we prepared azido linker (L=GDM $MeSO_2$) IL-15 using N_3-PEG_4-L(GDM $MeSO_2$)-CHO.

Preparation of MS~IL-15. A slurry of 1.4 mL of BCN-derivatized MSs containing 2.7 µmol BCN/mL in a 10 mL sterile syringe was washed with 5 x 7 mL of Buffer A. The azido-linker-IL-15 reaction mixture containing 1 µmol (~13 mg) of ~50% mono-alkylated IL-15 in 2 mL Buffer A was added to the syringe through a 0.22 µm sterile filter. The mixture was rotated end-over end at ambient temperature for 42 hours, and washed with 6 x 7 mL of Buffer A to remove free IL-15. The unreacted BCN groups were capped by treatment with 1 mL of 50 µmol/mL N_3-PEG_7 (Sigma Aldrich) for 24 hours and the MSs washed with 6 x 7 mL of Buffer A containing 30 mM methionine. MSs were equilibrated with Buffer A containing 30 mM methionine as an anti-oxidant and stored at 4°C. Protein content of the microspheres was determined by A_{280} in 5 mg aliquots of slurry after dissolution in 50 µL of 50 mM NaOH (IL-15; ε_{280}= 7240 M^{-1} cm^{-1}). The PEG content of the conjugate was determined following dissolution through $BaCl_2/I_2$ spectrophotometry. In the present case, in the 2.9 mL of packed gel product there was 975 nmol IL-15 indicating that 97% of the 1 µmol of N_3-linker-IL-15 reactant coupled to the MS-BCN. The PEG content was determined to be 7.9 mg/mL resulting in an IL-15/PEG ratio of 44 nmol IL-15/ mg PEG.

Similarly, we prepared MS_{GDM}~IL-15 by conjugating monoalkylated azido linker (GDM $MeSO_2$) IL-15 (40 mg) to BCN-derivatized MSs (4 µmol) with 80% yield. The concentration of the 1.6 mL of packed MSs was 19.7 mg/mL. The PEG content was determined to be 12.5 mg/mL and the IL-15/PEG ratio was 125 nmol IL-15/mg PEG.

IV. Characterization of MS~IL-15

In vitro release kinetics of MS~IL-15. The release kinetics of MS~IL-15 were determined under accelerated release conditions. Each of ~8 microcentrifuge tubes containing ~10 µL of the MS-IL-15 slurry were diluted with ~40 µL 100 mM NaBorate, 0.05% (v/v) tween-20, pH 9.4, and kept at 37°C. At intervals, samples were centrifuged at 15,000 x g for 2 min and A_{280} of the supernatants were measured using a NanoDrop spectrophotometer. The release rate was calculated by fitting the released A_{280} vs time to a first-order rate equation in GraphPad Prism 8.0, and the $t_{1/2}$ of the hydroxide catalyzed cleavage at pH 7.4 was calculated using the equation:

$$t_{1/2,\ pH\ 7.4} = t_{1/2,\ pH} \times 10^{(pH-7.4)}$$

Purity of IL-15 on MS-IL-15. Purity of the IL-15 conjugated to the microsphere was determined by monitoring the released proteins at pH 9.4, 37ºC, by HPLC. Here, 80 µL of a 350 µM solution was diluted 5-fold in 100 mM NaBorate, 0.05% (v/v) tween-20 pH 9.4, and was distributed into eight 1 mL centrifuge tubes and kept at 37ºC. At intervals spanning over 24 hrs, (~1 half-life of release) samples were centrifuged and 20 µL of the supernatants were analyzed by HPLC. The fraction of each released protein was determined as peak area/total peak areas, and log(peak area) of each component vs time were plotted. The y-intercept of the plot reveals the fraction of each protein present on the MSs at t=0, and the slope of the log IL-15 area vs t plot provides the rate at which IL-15 is degraded in the pH 9.4, 37ºC, buffer.

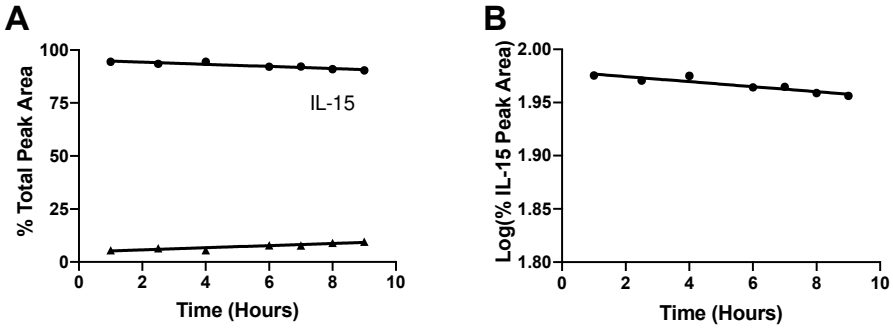

Figure S2. Purity of MS~IL-15. A) Purity of IL-15 bound to the microspheres. B) Rate of degradation of IL-15 at pH 9.4 37ºC. The MS~IL-15 slurry was washed two times and diluted in 125 mM sodium borate pH 9.4, and incubated at 37°C. Released proteins from the microspheres monitored by HPLC. The analysis shows >95% of the protein on the MSs is IL-15. IL-15 degrades in pH 9.4 buffer with a rate of 0.0024 hr^{-1}.

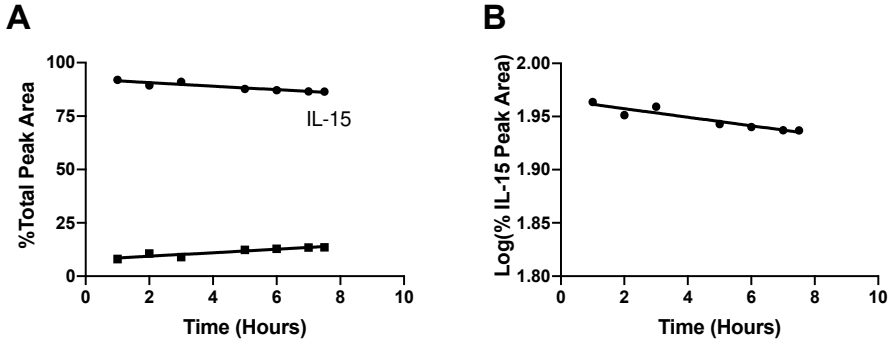

Figure S2B. Assessment of MS~IL-15: 1 month storage stability. A) Purity of IL-15 bound to the microspheres. B) Rate of degradation of IL-15 at pH 9.4 37ºC. The MS~IL-15 slurry was washed two times and diluted in 125 mM sodium borate pH 9.4, and incubated at 37°C. Released proteins from the microspheres monitored by HPLC. The analysis shows following 1 month of storage, >92% of the protein on the MSs is IL-15. IL-15 degrades in pH 9.4 buffer with a rate of 0.0040 hr^{-1}.

Bioactivity of IL-15$_{AP}$. To obtained IL-15$_{AP}$, 75 µL of the MS~IL-15 conjugate was washed 1x with PBS pH 7.4 and then diluted 10 fold in the same buffer. The reaction mixture was incubated at 37ºC for 10 days. The supernatant of the reaction mixture, containing IL-15$_{AP}$, was concentrated to 0.12 mg/mL (10 µM) using an Amicon Ultra 3,500 MW cut-off concentrator. The in vitro activity of IL-15$_{AP}$ was assessed using the U2OS cell-based assay kit for IL-2Rβγ binding.

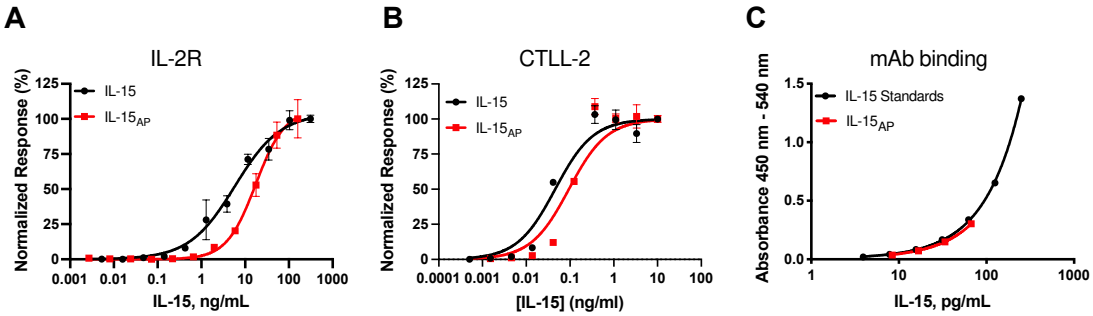

Figure S3. Bioactivity of IL-15$_{AP}$. WT IL-15 (●) and IL-15$_{AP}$ (■) were assayed for A) IL-2Rβγ binding via an U2OS cell-based assay and B) CTLL-2 cell proliferation. Data were fit to a four-parameter logistic model; points are averages ± SD. The EC$_{50}$ for IL-15 induced dimerization of IL-2Rβγ by IL-15 and IL-15$_{AP}$ was determined to be 5.8 ng/mL and 17 ng/mL, respectively. The EC$_{50}$ for IL-15 and IL-15$_{AP}$ CTLL-2 cell proliferation was 46 pg/mL and 94 pg/mL, respectively. C) Antibody binding of IL-15$_{AP}$ assessed via ELISA.

V. Stability studies of free IL-15

The *in vitro* stability of free IL-15 was assessed at pH 7.4, 37ºC and pH 6.0, 4ºC. IL-15 was buffer exchanged into either PBS pH 7.4 or 25 mM Na citrate, 500 mM NaCl, 0.05 tween-20 pH 6.0 using a MidiTrap G-25 desalting column and concentrated to a final concentration of 30 µM (0.385 mg/mL, 1 mL). The sample was divided into two aliquots (2x500µL), with one aliquot spiked with DNP-lysine (10 µM). Samples were incubated at either 37ºC for 10 days or at 4ºC for 28 days. Aliquots (40 µL) were removed over a predefined time course and stored at -80ºC until analysis by a cell-based IL-2Rβγ dimerization assay. DNP-lysine containing samples were analyzed using HPLC over the same time course.

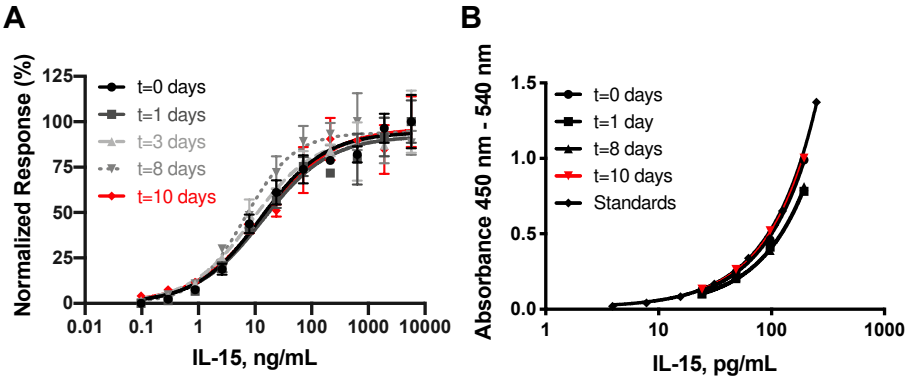

Figure S4. IL-15 bioactivity over 10 days stored at 37°C, pH 7.4. A) The bioactivity of IL-15 was measured by its ability to induce IL-2Rβγ receptor dimerization. Aliquots were taken from a master reaction mixture weekly and frozen at –80°C until all time points were collected. Data were fit to a four-parameter logistic model; points are averages ± SD. The EC_{50} for IL-15 induced dimerization of IL-2Rβγ was determined to 13 ng/mL for the t=0 day time point and 15 ng/mL for the t=10 day time point. B) Antibody binding of $IL\text{-}15_{AP}$ assessed via ELISA.

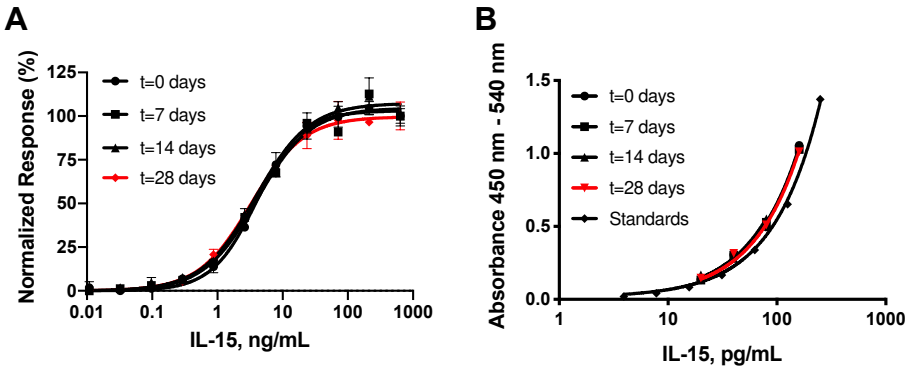

Figure S5. IL-15 bioactivity over 28 days stored at 4°C, pH 6.0**.** A) The bioactivity of IL-15 was measured by its ability to induce IL-2Rβγ receptor dimerization. Aliquots were taken from a master reaction mixture weekly and frozen at –80°C until all time points were collected. Data were fit to a four-parameter logistic model; points are averages ± SD. For all samples, the EC_{50} for IL-15 induced dimerization of IL-2Rβγ was determined to be between 3.3 and 4.0 ng/mL. B) Antibody binding of $IL\text{-}15_{AP}$ assessed via ELISA.

VI. Pharmacokinetic experiments

Preparation of dosing solutions. Dosing solutions were prepared by diluting the MS~IL-15 slurry (275 nmol/mL) in 25 mM Na citrate buffer pH 6.0 containing 500 mM NaCl, 0.05% tween-20 and 1.25% (w/v) hyaluronic acid. To confirm the IL-15 concentration, aliquots of the MS~IL-15 dosing solution(~20 µL) were diluted 5 fold in 50 mM NaOH and incubated for 1 hour at room temperature. Following dissolution of the microsphere conjugate, the reaction mixture (20 µL) was analyzed using standard HPLC methods. A standard curve was prepared using NCI IL-15

standards. IL-15 standards (0.25 mg/mL – 0.004 mg/mL) were prepared from 2-fold serial dilutions in 50 mM NaOH and incubated for 1 hour at room temperature. The concentration of IL-15 in each dosing solution was determined by peak area interpolation of the standard curve.

Pharmacokinetics of MS~IL-15 in immunocompetent mice. Syringes with fixed needles (27 G) were backfilled with the MS~IL-15 conjugate (100 µL). For studies that required various doses of MS~IL-15, serial dilutions were used to obtain the desired MS~IL-15 concentration. The contents of the syringes were administered either SC or IP to normal, male C57BL/6J mice. Blood samples were collected in EDTA collection tubes at -48, 4, 8, 24, 48, 96, 120, 168 and 240 hours from alternating groups of mice (n=3/group). Mice that received a second dose of MS~IL-15 were administered the second injection (100 µL, 50 µg IL15) at 240 hrs. Additional blood draws were taken at 248, 264, 288, 336, 360 and 408 hours. HALT protease inhibitor cocktail was added to all samples and the plasma frozen at –80°C until analysis by ELISA.

Pharmacokinetics of MS~IL-15 in immunodeficient mice. Male, NSG mice (n=3), 6-8 weeks in age, were injected sc with 100 µL of MS~IL-15 (50 µg IL-15) on day 0. Blood samples were collected in EDTA collection tubes containing HALT protease inhibitor at 24 h, 96 h, 168h, 240 h, 336 h, 408h, 504 h, and 576 h post injection. Plasma was prepared and stored at –80°C until analysis by ELISA.

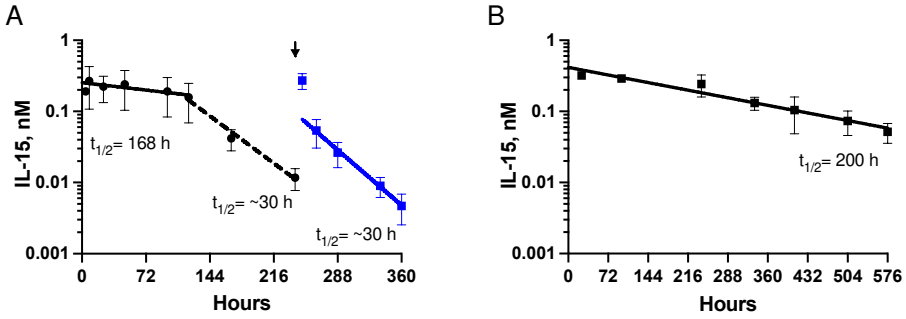

Figure S6. MS~IL-15 pharmacokinetics in immunocompetent and immunodeficient mice. A) C57BL/6J mice were administered SC MS~IL-$15_{50µg}$ on D0 and D10. The black arrow indicates the time of the second administration of MS~IL-15. B) NSG mice (n=6/group) were administered SC MS~IL-$15_{50µg}$ on D0. Plasma was analyzed using R&D System hIL-15 Quantikine ELISA.

VII. Anti-drug antibody ELISA

The presence of anti-rhIL-15 antibodies was assayed for following previously published methods with the following noted exceptions (*1*) . The standard curve for anti-human IL-15 (AF315, R&D Systems) was determined in the presence and absence of 125 pg/mL (10 pM) and 4,000 pg/mL (310 pM) exogenous rhIL-15. Test samples were diluted 9 fold in PBS/1% BSA. Controls were prepared in C57B/6J plasma diluted 9 fold in PBS/1% BSA. All samples and controls were incubated overnight at 4°C. After the assay was developed with p-nitrophenol phosphate (1mg/mL, 100 µL) for 1 hour at 37°C, the absorbance at 405 nm was recorded using a Spectramax i3 plate reader. The limit of detection for an undiluted sample was 195 ng/mL.

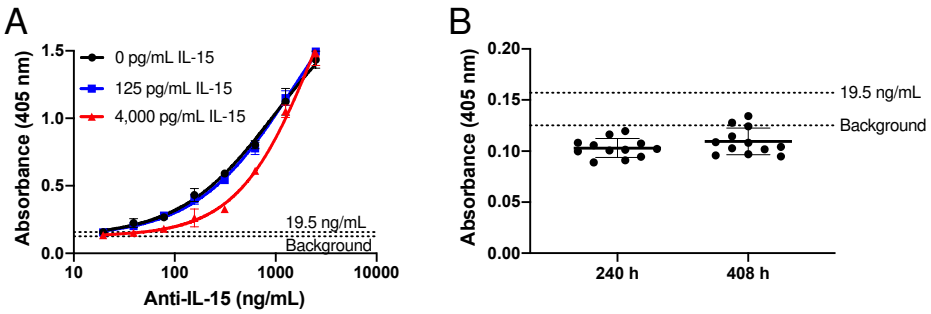

Figure S7. Anti-rhIL-15 antibodies are not detected in mouse plasma. A) Calibration curve for anti-IL-15 antibodies. B) Analysis of test samples for anti-rhIL-15 antibodies (n=12). An affinity purified goat anti-human IL15 (AF315, R&D Systems) was used to define the standard curve in the presence and absence of 125 pg/mL (10 pM) or 4,000 pg/mL (310 pM) exogenous rhIL-15.

VIII. Pharmacodynamics experiments

Pharmacodynamics of MS~IL15 in Spleen, lymph nodes and PBMCs. Normal, male C57black mice (n=18/group) received either a single injection of MS~IL-$15_{50\mu g}$ sc or five daily injection of rhIL-15 (5 µg, QDx5) IP. On days 2, 5, 7, 14, 21 and 28, 3 mice were sacrificed from each group. The spleen and lymph nodes (Superficial cervical, deep cervical, mediastinal, axillary, brachial, mesenteric and inguinal) were harvested and single cell suspensions were prepared. Blood, splenocytes and lymph node lymphocytes were immunophenotyped to quantitate NK cells, B cells, $CD4^+$, $CD8^+$, $CD44^{hi}CD8^+$ and γδ T cells, as well as their proliferating subsets. Prior to the start of the study, five untreated mice were sacrificed to determine baseline cell numbers in the spleen, lymph node and blood. The total AUC for each cell phenotype was determined using Prism. Then, the baseline cell count x 28 was subtracted to yield the AUC_{28d}.

Dose comparison of single or multiple doses of IL-15 to MS~IL-15. A single dose of 5 µg, 10 µg, 25 µg or 50 µg rhIL-15, multiple daily doses of IL-15 (5 µg), a single dose of 10 µg RLI, or two doses of 2 µg RLI (D0 or D2) were administered ip (100 µL) to normal, male C57Black mice (n=4-5/group). An additional group of mice (n=10) received 50 µg MS~IL-15 (Mod: std $MeSO_2$) administered sc (100 µL). Blood samples were drawn on day -2, 2, 5, 7, 14, 21 and 28 and immunophenotyped with an Attune NxT flow cytometer to quantitate B cells, NK cells, CD3, CD4, CD8, and CD44 expressing cells. The total AUC for each cell phenotype was determined using Prism. Then, the baseline cell count x 28 was subtracted to yield the AUC_{28d}.

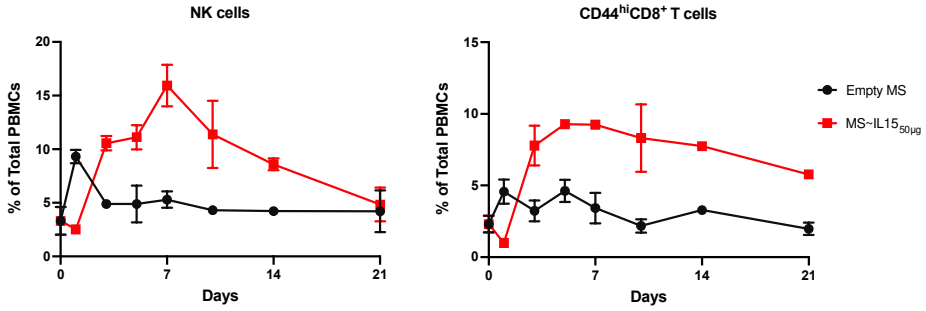

Figure S8. Immune cell response of MS~IL-$15_{50µg}$ compared to empty microspheres. The percentage of NK cells and $CD44^{hi}CD8^{+}$ T cells in PBMCs were measure over 21 days. Mice were administered a single SC dose of MS~IL-$15_{50µg}$ or empty MS (n=3/group).

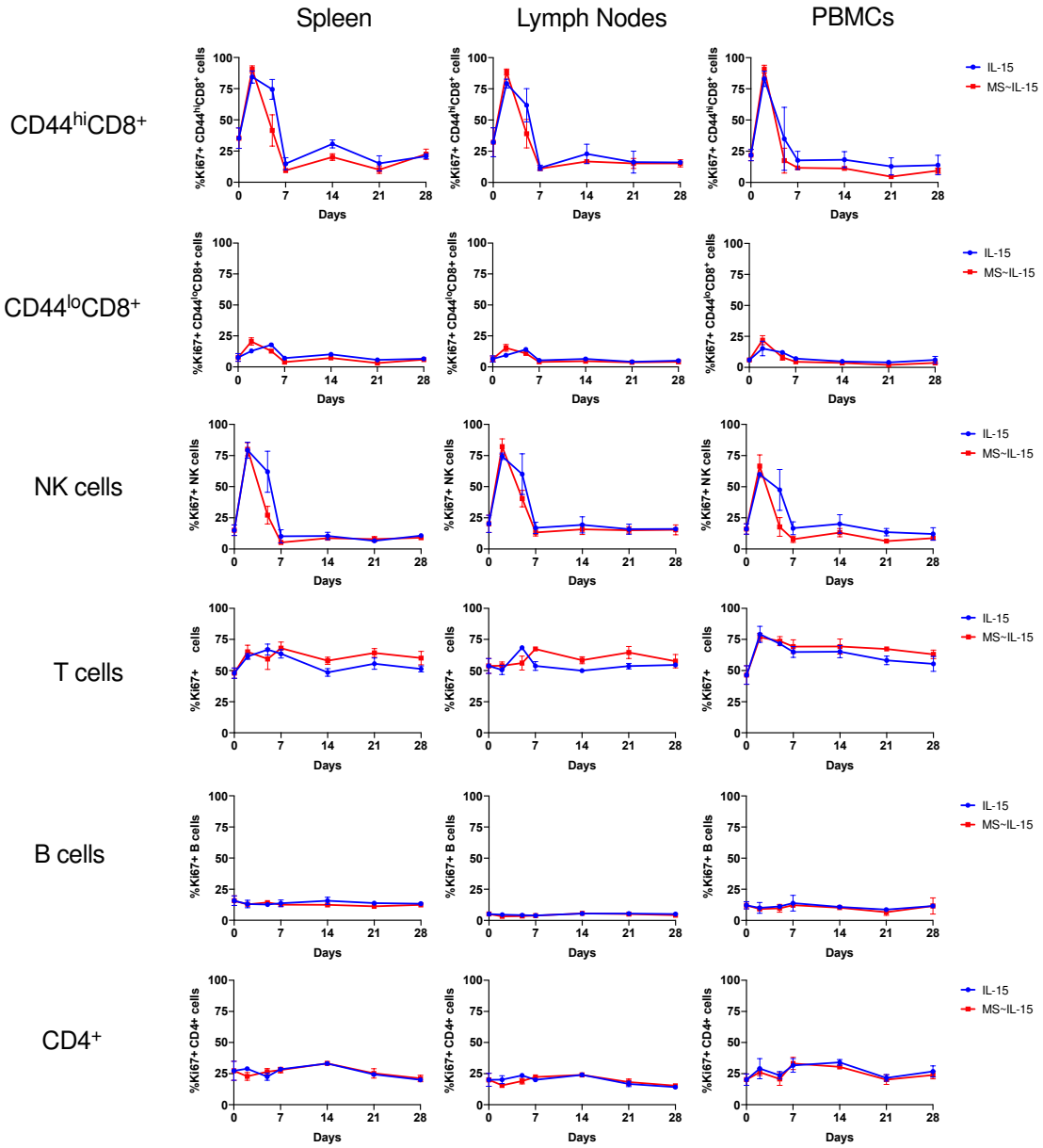

Figure S9A. Proliferation of target immune cells by MS~IL-$15_{50\mu g}$ and 5 µg IL-15 QD x 5 measured over 28 d. Enumeration of NK, $CD8^+$, $CD44^{hi}CD8^+$ T and γδ T cells in the spleen, lymph nodes and blood of mice treated with 50 µg MS~IL-15 (■) or 5 µg IL-15 QD x 5 (●).Tissues were collected (n=3 mice/time point) at 0, 2, 5, 7,14, 21 and 28 d and analyzed for specified cells.

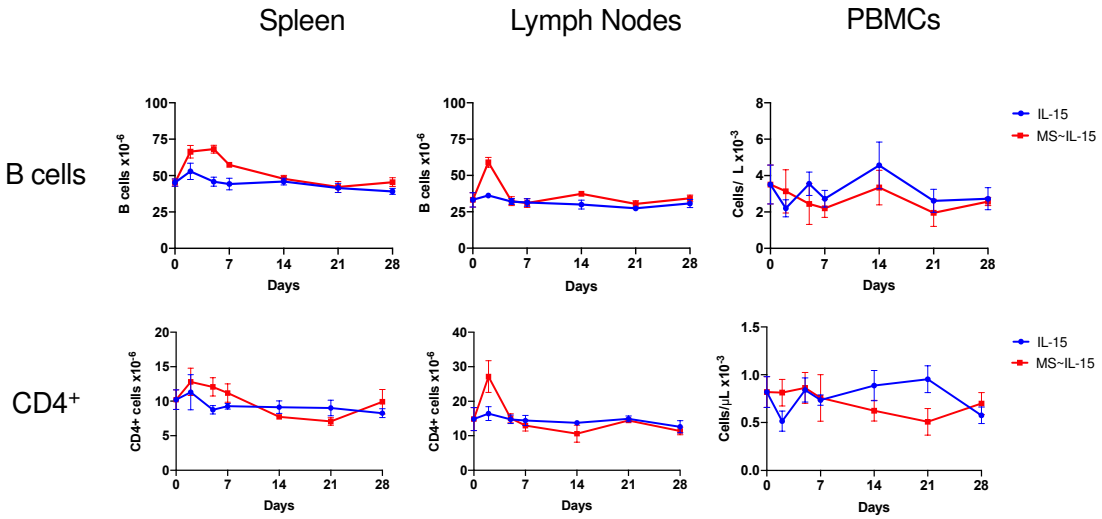

Figure S9B. Immune cell expansion by MS~IL-15$_{50µg}$ over 28 d. Enumeration of CD4$^+$ and B cells at 0, 2, 5, 7,14, 21 and 28 d in the spleen, lymph nodes and PBMCs of mice (n=3/point/group) treated with SC MS~IL-15$_{50µg}$ (■) or IP 5 µg IL-15 QD x 5 (●).

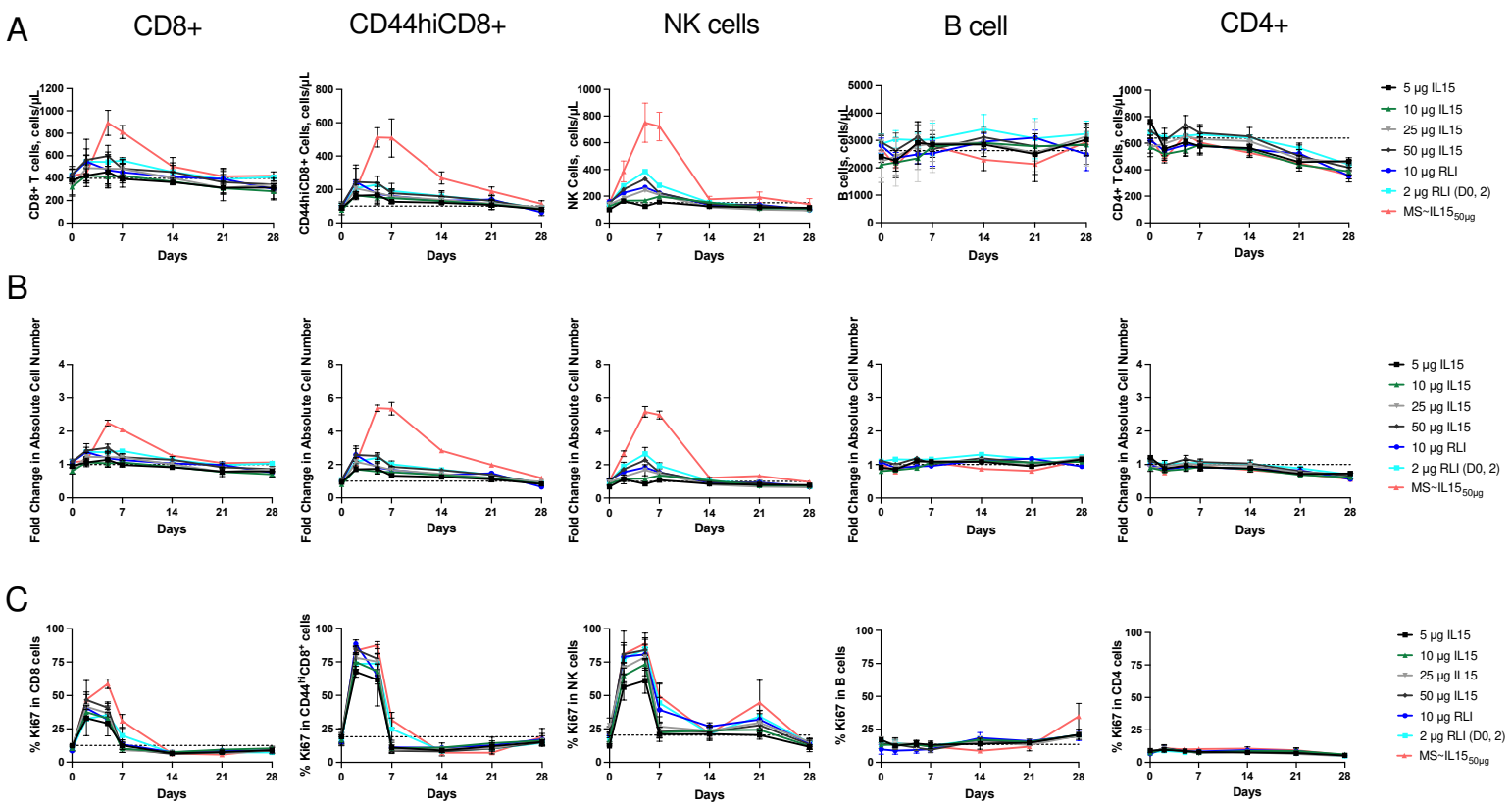

Figure S10. MS~IL-15$_{50µg}$ has significant increase in NK cells and CD44^{hi}CD8^{+} T cells compared to rhIL-15 and RLI. A) Absolute cell number B) Fold change in absolute cell number and C) Percentage of proliferating CD4^{+}, CD8^{+}, CD44^{hi}CD8^{+} , NK, and B cells. Mice were administered a single ip dose of rhIL-15 (5 – 50 µg), RLI (10 µg), two IP doses of RLI (2 µg) separated by 48 h, or a single SC dose of MS~IL-15$_{50µg}$ (n=4-5/group).

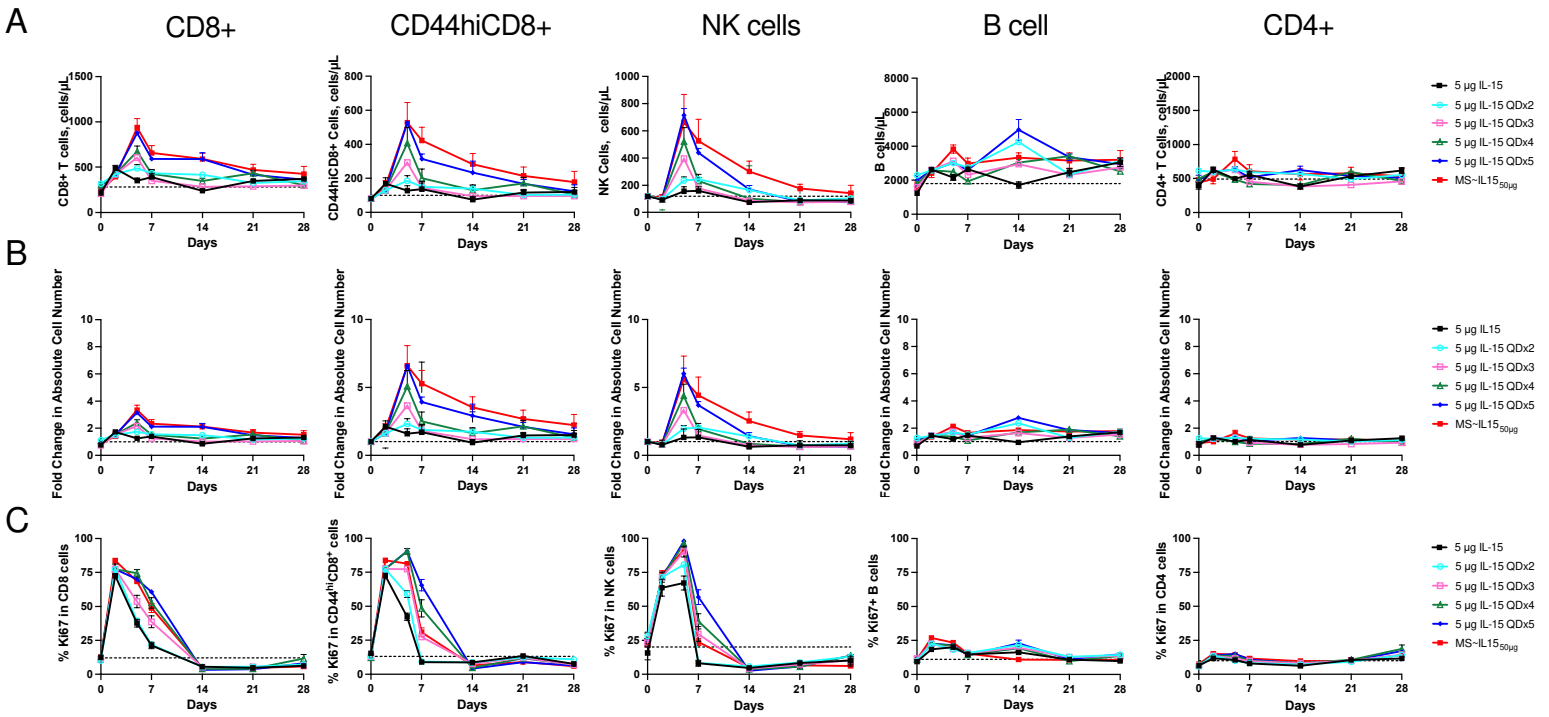

Figure S11. PD response of multiple doses of IL-15 compared to MS~IL-15$_{50µg}$. A) Absolute cell number B) Fold change in absolute cell number and C) Percentage of proliferating CD4^{+}, CD8^{+}, CD44^{hi}CD8^{+}, NK, and B cells. Mice were administered sequential daily IP doses of 5 µg rhIL-15 (QDx1 – QDx5) (n=5/group)

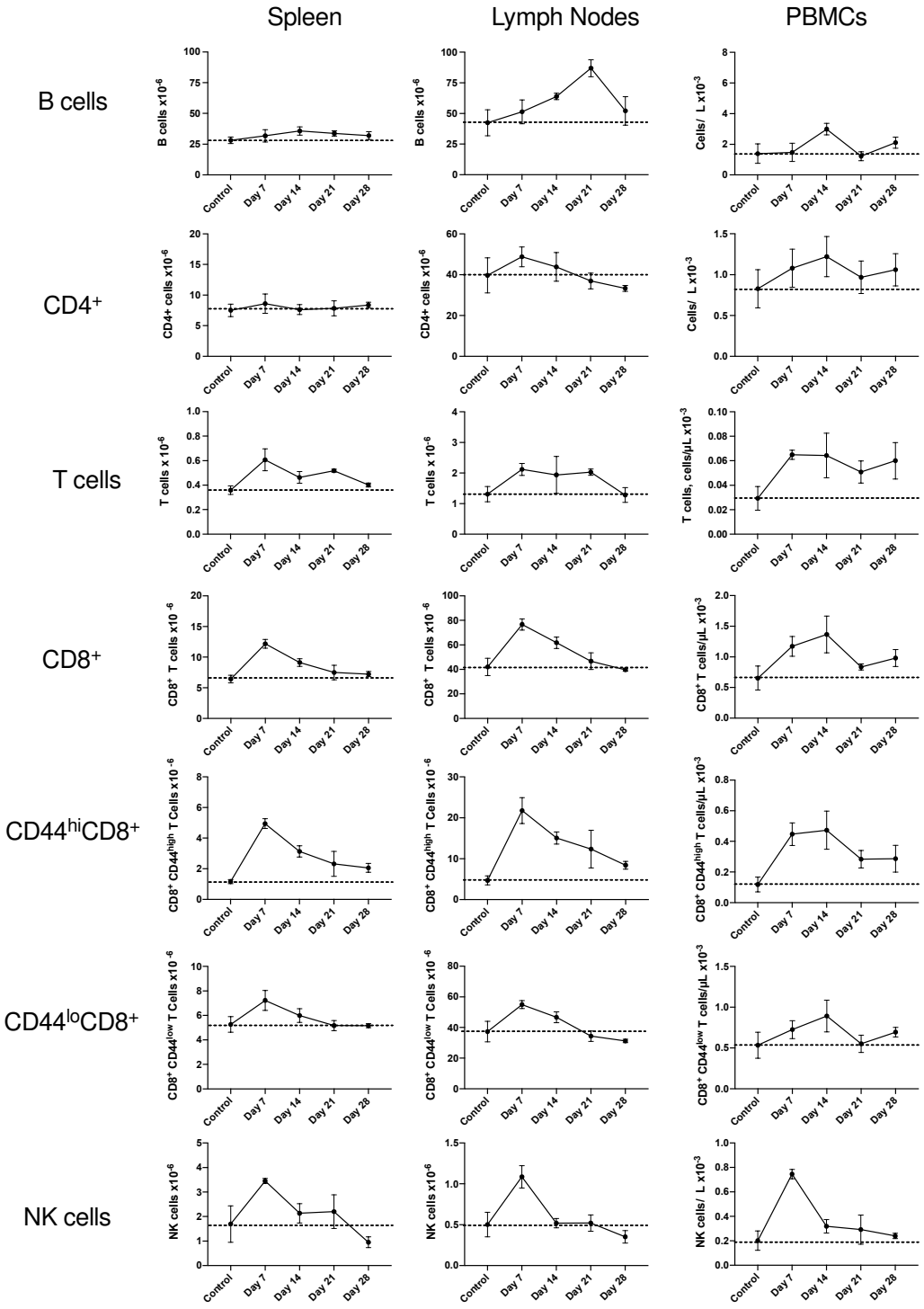
Spleen
Lymph Nodes
PBMCs
B cells
CD4+
T cells
CD8+
CD44hiCD8+
CD44loCD8+
NK cells
B cells x10-6
Cells/ L x10-3
CD4+ cells x10-6
T cells x 10-6
T cells, cells/µL x10-3
CD8+ T cells x10 -6
CD8+ T cells/µL x10-3
CD8+ CD44high T Cells x10 -6
CD8+ CD44high T cells/µL x10-3
CD8+ CD44low T Cells x10 -6
CD8+ CD44low T cells/µL x10-3
NK cells x10-6
NK cells/ L x10-3
Control
Day 7
Day 14
Day 21
Day 28

Figure S12. Absolute cell number immune cell expansion by MS_{GDM}~IL-$15_{50\mu g}$ measured over 28 d. Enumeration of B cells, NK cells, $CD4^+$, $CD8^+$, $CD44^{hi}CD8^+$, $CD44^{lo}CD8^+$and $\gamma\delta$ T cells in the spleen, lymph nodes and blood of mice treated with 50 µg MS_{GDM}~IL-15. The dotted line represents the mean value of pre-treatment controls from 3 untreated mice. Tissues were collected (n=3 mice/time point) at 0, 7,14, 21 and 28 d and analyzed for specified cells.

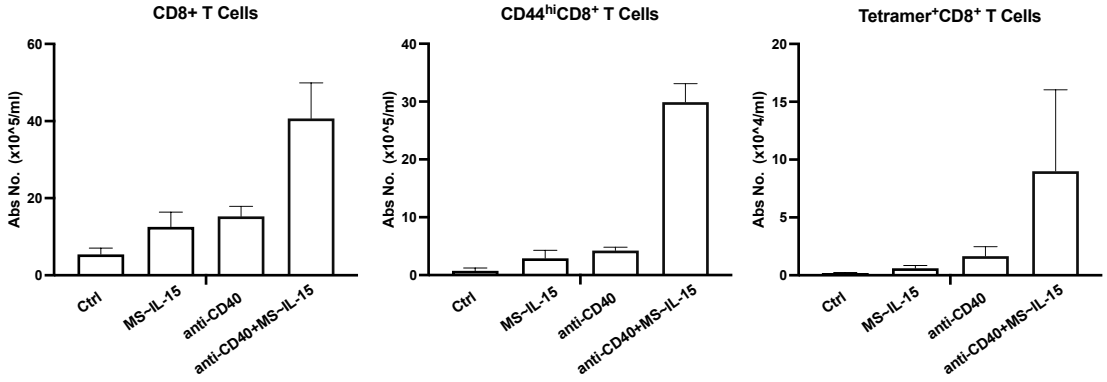

Figure S13. Absolute cell number CD8+ T cell expansion 16 days post treatment in C57BL/6J mice bearing TRAMP-C2 tumors on both flanks. Mice were treated with a single dose of SC MS~IL-$15_{50\mu g}$, IT anti-CD40 mAb (20 µg/10µl on d 0, 3, 7, and 10) in the right-flank tumor or the combination of MS~IL-$15_{50\mu g}$ plus anti-CD40. The control group was injected with PBS. Data represents average ± SD (n=2-4/group).

Table S2. AUC_{28d} for MS_{GDM}~IL-$15_{50\mu g}$ PD effect on target immune cells.

Marker	Tissue	pre-dose control, cells [A]	Duration, d	AUC, cells* d [B]
		mean ± SD		
$NK1.1^+$	spleen	1.7 ± 0.7	14	16
	ln	0.50 ± 0.15	14	3.8
	PBMC	0.18 ± 0.14	14	4.5
$CD8^+$	spleen	6.4 ± 0.62	21	69
	ln	42 ± 7	21	410
	PBMC	0.63 ± 0.18	21	11
$CD44^{hi}CD8^+$	spleen	1.2 ± 0.2	28	52
	ln	4.7 ± 1.1	28	260
	PBMC	0.11 ± 0.10	28	6.5
$TCR\gamma\delta^+$	spleen	0.36 ± 0.04	14	3.7
	ln	1.3 ± 0.2	28	15
	PBMC	0.03 ± 0.01	28	0.75

[A] Control values are cells * 10^{-6} for spleen and lymph nodes (ln), and cells/µl *10^{-3} for PBMCs.
[B] AUC values are cells * 10^{-6} * d for spleen and ln, and cells/µl *10^{-3} *d for PBMCs.

IX. Therapeutic studies of MS~IL15

TRAMP-C2 model. The TRAMP-C2 cell line, derived from a prostate tumor of the TRAMP mouse, was administered to four groups of wild-type C57 black mice on both flanks. When the tumors volumes reached 40-60 mm^3, treatment began. The treatment for each group was as follows: 1) empty microspheres, 2) anti-CD40 3) MS~$IL15_{50\mu g}$ 4) MS~$IL\text{-}15_{50\mu g}$ plus anti-CD40. Anti-CD40 (20 µg) was injected interlesionally in the right flank tumors on day 0, 3, 7 and 10. The impact on the time-course development of tumor size was determined for both the right side anti-CD40 injected and the left side untreated tumor. Kaplan-Meier mouse survival plots were generated based on the survival of mice in each group. The tumor size was measured in two orthogonal dimensions twice per week and survival of the mice was monitored throughout the experiment based on humane endpoint criteria. Tumor volume calculations were obtained from caliper measurements using the formula V = (W/2 x L/2).

Mouse Model of MET-1 leukemia. Six to eight-week-old female NOD.Cg-Prkdcscid/J mice (#001303) were purchased from the Jackson Laboratory (Bar Harbor, ME). MET-1 Leukemia was established by IP injection as previously described (*7*). Briefly, viably frozen or freshly isolated MET-1 from splenocytes ($2x10^7$ cells) was injected IP and the therapy was started when sIL-2Rα levels in mice serum were approximately 1,000 pg/ml which was 10–14 days after tumor inoculation. MS~$IL\text{-}15_{50\mu g}$ was injected on one occasion subcutaneously. CCR4 antibody (Mogamulizumab, 100 µg) was given via IP injection 2 days after MS~$IL\text{-}15_{50\mu g}$ injection and then weekly for 4 weeks alone or in combination with MS~$IL\text{-}15_{50\mu g}$ at the same dose and dosing schedule. The percentage and absolute number of NK cells were measured, and the survival of the mice was recorded.

X. Animal Welfare Statement

Animal experiments performed at the NIH/NCI were approved by the NCI Animal Care and Use Committee and were performed in accordance with NCI Animal Care and Use Committee guidelines. All other animal handling and care was performed by MuriGenics (Vallejo, CA) and Explora Biolabs (San Francisco, CA). All experiments conformed to IACUC recommendations.

XI. Derivation of Time Over Target Equation

For simple first-order clearance, the concentration of drug in the plasma at time t is given by:

$$C(t) = (Dose/V_d)\bullet exp(-k_e t)$$

where V_d = volume of distribution and k_e = the elimination rate constant. To calculate how long a given dose will provide plasma concentrations above a target concentration, C_{min} (i.e., the "time-over-target" = TOT):

$$C_{min} = (Dose/V_d)\bullet exp(-k_e t_{min})$$

$$TOT = t_{min} = [ln(Dose/(C_{min}\bullet V_d))]/k_e$$

Thus, there is a logarithmic relationship between dose and TOT:

$$TOT = A\bullet ln(Dose) - B$$

where A and B are constants determined by C_{min}, V_d, and k_e

$$A = 1/k_e$$

$$B = (ln(C_{min}\bullet V_d))/k_e$$

The change in time-over-target between two doses related as $Dose_2 = x\bullet Dose_1$ (i.e., an x-fold change in the dose) is thus given as

$$DTOT = TOT_2 - TOT_1 = A\bullet[ln(Dose_2) - ln(Dose_1)] = A\bullet ln(Dose_2/Dose_1)$$

$$DTOT = ln(x)/k_e = t_{1/2}\bullet ln(x)/ln(2)$$

The ratio of TOT_2/TOT_1 (i.e., the fold increase in TOT for a given fold increase in dose x) is thus

$$TOT_2/TOT_1 = (TOT_1 + DTOT)/TOT_1 = 1 + DTOT/TOT_1$$

Which simplifies to

$$TOT_2/TOT_1 = 1 + ln(x)/ln(Dose_1/C_{min}V_d)$$

If we are interested only in the relative fold-change in TOT with a certain fold-increase in dose X, this simplifies further to

$$TOT_2/TOT_1 = 1 + ln(x)/Z$$

$$\text{Where } Z = ln(Dose_1/C_{min}V_d)$$

XII. Supplemental discussion for the tolerance of MS~IL-15

The purpose of this study was to evaluate the toxicity/tolerability of MS~IL-15, when administered as subcutaneous (SC) injections on Day 1 and Day 15 to male C57BL/6 mice. Each treatment group (Groups 1–3) was comprised of six male C57BL/6 mice. Mice were administered the vehicle control (Group 1) or 0.15 or 0.50 mg/animal/injection MS~IL-15 (Groups 2 or 3, respectively) once on Day 1 (Injection Site #1) and once on Day 15 (Injection Site #2) via subcutaneous injection at a dose volume of 0.1 mL/injection. Clinical observations were recorded at least once daily, approximately 1 hour post-dose on dosing days, and on the day of necropsy. Physical examinations were conducted at randomization. Body weight measurements were taken for randomization, twice weekly, and prior to necropsy. Terminal plasma samples were collected from all groups at necropsy for bioanalysis of MS~IL-15. Blood samples for the evaluation of hematology and clinical chemistry endpoints were collected on Day 28 from all groups. Following blood sample collections, necropsy was conducted. Tissues were collected and evaluated grossly, select organs were weighed, and tissues were fixed for microscopic evaluation. Tissues were subsequently processed and evaluated microscopically.

All mice survived until the scheduled sacrifice. Compared to vehicle controls, there were no test article-related changes in body weights. There were no test article-related clinical pathology, organ weight, or macroscopic findings. Injection site swelling occurred across all groups with an overall exacerbated incidence following the second injection and a noteworthy increase in incidence at 0.50 mg/animal/injection, compared to vehicle controls, which persisted through Day 28. These changes were indicative of a vehicle-effect with test article exacerbation in MS~IL-15 groups.

At ≥0.15 mg/animal/injection, there was test article-related minimal to moderate subcutaneous granulomatous inflammation (Site 1, 0.15 mg/animal/injection - 4/6, 0.50 mg/animal/injection - 1/6, Site 2, 0.15 mg/animal/injection – 0/6, 0.50 mg/animal/injection - 1/6) that was not dose-dependent. All instances of test article-related granulomatous inflammation were associated with the microsphere vehicle. The identification of granulomatous inflammation in controls indicated that the microsphere vehicle contributed to inflammation to some degree. However, severity of inflammation was substantially higher in both Groups 2 and 3, which supported a test article-related effect. There was a single incidence of test article-related mild subcutaneous myofiber degeneration/regeneration at 0.15 mg/animal/injection.

In conclusion, MS~IL-15-related findings included minimal to moderate subcutaneous granulomatous inflammation (associated with the microsphere vehicle), one occurrence of mild myofiber degeneration/regeneration (0.15 mg/animal/injection only), and slight injection site swelling. Because there were no MS~IL-15 related changes in body weights and no dose-dependent microscopic differences between the 0.15 and 0.50 mg/animal/injection groups, MS~IL-15, administered every two weeks at 0.15 or 0.50 mg/animal/injection, was generally tolerated by male C57BL/6 mice, under the conditions of this study.

XIII. Supplemental References

1. K. C. Conlon, E. Lugli, H. C. Welles, S. A. Rosenberg, A. T. Fojo, J. C. Morris, T. A. Fleisher, S. P. Dubois, L. P. Perera, D. M. Stewart, C. K. Goldman, B. R. Bryant, J. M. Decker, J. Chen, T. A. Worthy, W. D. Figg, Sr., C. J. Peer, M. C. Sneller, H. C. Lane, J. L. Yovandich, S. P. Creekmore, M. Roederer, T. A. Waldmann, Redistribution, hyperproliferation, activation of natural killer cells and CD8 T cells, and cytokine production during first-in-human clinical trial of recombinant human interleukin-15 in patients with cancer. *J Clin Oncol* **33**, 74-82 (2015).
2. E. Mortier, A. Quemener, P. Vusio, I. Lorenzen, Y. Boublik, J. Grotzinger, A. Plet, Y. Jacques, Soluble interleukin-15 receptor alpha (IL-15R alpha)-sushi as a selective and potent agonist of IL-15 action through IL-15R beta/gamma. Hyperagonist IL-15 x IL-15R alpha fusion proteins. *J Biol Chem* **281**, 1612-1619 (2006).
3. H. Perdreau, E. Mortier, G. Bouchaud, V. Sole, Y. Boublik, A. Plet, Y. Jacques, Different dynamics of IL-15R activation following IL-15 cis- or trans-presentation. *Eur Cytokine Netw* **21**, 297-307 (2010).
4. D. F. Nellis, D. F. Michiel, M. S. Jiang, D. Esposito, R. Davis, H. Jiang, A. Korrell, G. C. t. Knapp, L. E. Lucernoni, R. E. Nelson, E. M. Pritt, L. V. Procter, M. Rogers, T. L. Sumpter, V. V. Vyas, T. J. Waybright, X. Yang, A. M. Zheng, J. L. Yovandich, J. A. Gilly, G. Mitra, J. Zhu, Characterization of recombinant human IL-15 deamidation and its practical elimination through substitution of asparagine 77. *Pharm Res* **29**, 722-738 (2012).
5. G. Soman, X. Yang, H. Jiang, S. Giardina, V. Vyas, G. Mitra, J. Yovandich, S. P. Creekmore, T. A. Waldmann, O. Quinones, W. G. Alvord, MTS dye based colorimetric CTLL-2 cell proliferation assay for product release and stability monitoring of interleukin-15: assay qualification, standardization and statistical analysis. *J Immunol Methods* **348**, 83-94 (2009).
6. E. L. Schneider, B. R. Hearn, S. J. Pfaff, S. D. Fontaine, R. Reid, G. W. Ashley, S. Grabulovski, V. Strassberger, L. Vogt, T. Jung, D. V. Santi, Approach for Half-Life Extension of Small Antibody Fragments That Does Not Affect Tissue Uptake. *Bioconjug Chem* **27**, 2534-2539 (2016).
7. K. E. Phillips, B. Herring, L. A. Wilson, M. S. Rickford, M. Zhang, C. K. Goldman, J. Y. Tso, T. A. Waldmann. IL-2Ralpha-Directed Monoclonal Antibodies Provide Effective Therapy in a Murine Model of Adult T-Cell Leukemia by a Mechanism other than Blockade of IL-2/IL-2Ralpha Interaction. *Cancer Research*. **60**, 6977-6984 (2000).